

INVESTIGATION OF FRACTURE MECHANICAL PERFORMANCE OF
NODULAR CAST IRON AND WELDED JOINTS WITH PARENT-
MATERIAL-LIKE WELD METAL

G. Pusch* and W. Baer*

The focus of the investigations was the determination of fracture mechanical characteristics and crack resistance curves of the J-Integral and CTOD concept by application of the partial unloading compliance technique and D.C. potential drop technique. Furthermore, a method for measurement of critical stretch-zone values by use of a laser roughness measurement system was established. The results of the fracture mechanical investigations show a close correlation between crack resistance curves as well as crack initiation values and graphite morphology parameters.

INTRODUCTION

The determination of fracture mechanical characteristics of ductile cast iron materials and their welded joints, taking into account the increasing application of welded castings, is the basis for an assessment of the influence of graphite morphology (size, shape, distance of the particles) and different microstructural components in the weld area in dependence on the applied stress. Furthermore, this is a prerequisite for a fracture mechanical safety analysis of castings containing cracks or crack-type stress concentration spots.

EXPERIMENTS

The materials studied are ferritic nodular cast iron GGG-40 with varying graphite morphology and welded joints of these materials with parent-material-like weld metal (i.e. the weld metal is similar to the parent material, with a ferritic matrix

* Institute of Materials Engineering, Freiberg University of Mining and Technology

and graphite nodules). In addition three types of ferritic cast iron GGV-30 with vermicular graphite shape were examined.

The welded joints generated by application of an optimized welding and in-situ heat treatment technology (1) are characterised by 14 % strength-over-matching of the parent-material-like weld metal, clearly smaller graphite particles in the weld metal due to the solidification conditions, and a ferritic matrix in the weld metal and the parent material (TABLE 1). No brittle structural components have been detected in the heat affected zone (HAZ).

TABLE 1 - Mechanical Properties and Graphite Morphology Parameters of the investigated Materials

| Material | σ_U [MPa] | $\sigma_{0,2}$ [MPa] | A [%] | f | λ [μm] | \varnothing [μm] | d [μm] |
|---|---------------------|-------------------------|----------|------|--------------------------------|------------------------------------|------------------------|
| GGV-30/4 | 295 | 240 | 5 | 0,32 | 37 | 12 | - |
| GGV-30/6 | 325 | 255 | 8 | 0,44 | 51 | 17 | - |
| GGG-40/1AZ | 416 | 277 | 24 | 0,85 | 54 | 23 | 35 |
| GGG-40/3AZ | 387 | 278 | 25 | 0,70 | 102 | 54 | 50 |
| GGG-40/4AZ | 381 | 265 | 21 | 0,65 | 93 | 48 | 59 |
| Welded Joint with Parent-Material-like Weld Metal | | | | | | | |
| GGG-40/2AZ | 393 | 259 | 26 | 0,84 | 58 | 21 | 30 |
| GGG-40/2WEZ | 408 | 264 | 24 | 0,83 | 50 | 24 | 28 |
| GGG-40/2GW | 408 | 264 | 24 | 0,80 | 52 | 21 | 28 |
| GGG-40/2SG | 441 | 301 | 23 | 0,70 | 16 | 7 | 18 |

A detailed characterization of the graphite morphology (TABLE 1) was carried out by means of f (shape parameter that approximately describes the notch effect of the particle, $f \leq 1$, $f=1$ spherical shape, $f < 1$ deviation from spherical shape), λ (mean distance of graphite particles), \varnothing (mean diameter of particles), d (ferrite grain size) where the notation is as follows: A...elongation; "/2AZ" - /2...internal number, AZ...original state without welding procedure, GW...parent material after welding procedure and post weld heat treatment, WEZ...HAZ, SG...weld metal. Fracture Mechanics. The determination of fracture mechanical characteristics of the original states and the welded joints by application of the J-integral and CTOD concepts was carried out by use of 20% sidegrooved SENB specimens ($a/W=0.5$, thickness $B=10$ mm, width $W=20$ mm), according to the ESIS P2-92 document, under static load and 4-pt bend. Computer aided testing and analysis

of the crack resistance curves (J-R and δ -R curves) were performed by application of the partial unloading compliance technique. The J_i^{BL} and δ_i^{BL} values were determined at the point of intersection of the calculated J-R and δ -R curves with the analytical blunting line and the technical crack initiation values $J_{0.2}$ and $\delta_{0.2}$ at a value of $\Delta a = 0.2$ mm of stable crack growth. Simultaneously, the D.C. potential drop technique was applied for experimental determination of stable crack initiation and provided reproducible J_i^{EP} and δ_i^{EP} crack initiation values.

Stretch Zone Measurement. A new method for stretch zone measurement with a laser instrumented device for the measurement of surface roughness by the profile method (2) was practised as an alternative to the SEM technique and adapted to the analysis of ferritic nodular cast iron.

The fracture surface is scanned in 70 profiles across the specimen thickness with an resolution of 1 micron horizontal and 0.1 microns vertical. With the help of special analyzing software the profile data can be processed and it is possible to determine the critical values of stretch zone width (SZB_c) and height (SZH_c) at once (FIGURE 1). The combination of the 2 dimensional profiles provides a 3 dimensional outline of the fracture surface (FIGURE 2). This method offers handling and time advantages and was justified by comparison measurements with SEM. In the analysis of nodular cast iron arises a number of material-specific difficulties such as the relatively strong roughness of the fatigue crack surface due to the graphite particles, non-uniform stretch zone formation over the specimen thickness, and a possible local terrace-shaped image of the stretch zone. Additional information like the fatigue crack length was found to be useful for a better reproducible determination of stretch zone parameters.

RESULTS AND DISCUSSION

The J-R crack resistance curves (FIGURE 3) reflect the increasing crack growth resistance of ferritic nodular cast iron with rising distance of graphite particles as well as the detrimental influence of the higher notch effect of the vermicular graphite. In the investigated welded joints of GGG-40/2AZ, the heat affected zone showed a microstructure-related crack growth resistance comparable to that of the parent material, as well as a clearly lower crack initiation toughness in the weld metal defined by the physical and technical crack initiation values (TABLE 2). A comparison of strength values of the original state, parent material and weld metal shows their increase for the weld metal depending on microstructure whereas the deformation characteristics remain nearly constant.

Obviously, there is no correlation between the values of the critical stretch zone width and the graphite morphology parameters. The crack initiation toughness values based on the critical stretch zone width values are clearly lower than the technical values $J_{0.2}$ and show good agreement with the other physical crack initiation values J_i^{BL} . The experimental determination of physical crack

TABLE 2 - Fracture Mechanical Characteristics and critical Stretch-Zone Width

| Material | J_i^{BL} [kJm ⁻²] | J_i^{EP} [kJm ⁻²] | J_i^{SZBc} [kJm ⁻²] | $J_{0.2}$ [kJm ⁻²] | SZBc [μm] |
|--|------------------------------------|------------------------------------|--------------------------------------|-----------------------------------|--------------|
| GGV-30/4 | 8 | 15 | - | 19 | - |
| GGV-30/6 | 11 | 20 | 13 | 28 | 23 |
| GGG-40/1AZ | 23 | 28 | 25 | 41 | 21 |
| GGG-40/3AZ | 40 | 56 | 40 | 75 | 25 |
| GGG-40/4AZ | 35 | 52 | 36 | 68 | 23 |
| Welded Joint with Parent-Material-Like Weld Metal | | | | | |
| GGG-40/2AZ | 30 | 34 | 30 | 47 | 21 |
| GGG-40/2WEZ | 28 | 32 | 30 | 46 | 24 |
| GGG-40/2GW | 35 | 42 | 36 | 49 | 27 |
| GGG-40/2SG | 23 | 21 | 23 | 29 | 17 |

initiation characteristics by use of the D.C. potential drop technique is possible at a justifiable cost and offers the advantage, especially with the evaluation of welded joints, that the influence of a possible crack deviation (e.g. from the HAZ into the weld metal) is eliminated by a restriction of the amount of stable crack growth. For the investigated materials these J_i^{EP} values fit in between the J_i^{BL}/J_i^{SZBc} and $J_{0.2}$ values. The crack initiation and propagation resistance of ferritic ductile cast iron is dominated by the ductile matrix. The strength overmatching of the weld metal is accompanied by lower crack initiation toughness values that are due to the small size of the graphite particles in spite of the beneficial effect of a small ferrite grain size on toughness. A smaller mean distance between the graphite particles correlates with its smaller size. This and the direct proportionality between the critical crack tip opening δ and the size of particles resulting from theoretical models are also considered to be the reason of the loss of toughness with decreasing particle size. Concerning the shape of graphite particles, it should be noticed that a deviation from the spherical shape represented by the shape factor also leads to a decrease of crack initiation toughness due to the additional increase of the notch effect (FIGURE 4).

REFERENCES

- (1) Pusch, G.; Baer, W. und Michael, A.: Beitrag zur Optimierung artgleicher Schweißverbindungen des ferritischen Gußeisenwerkstoffes GGG-40, Gießerei 80 (1993) 7, S. 227-231
- (2) Louis, H. "Stretchzonen-Bestimmung mit Hilfe eines modifizierten Tastschnittverfahrens", Forschungsbericht Lo 223/8-2, Universität Hannover, 1991

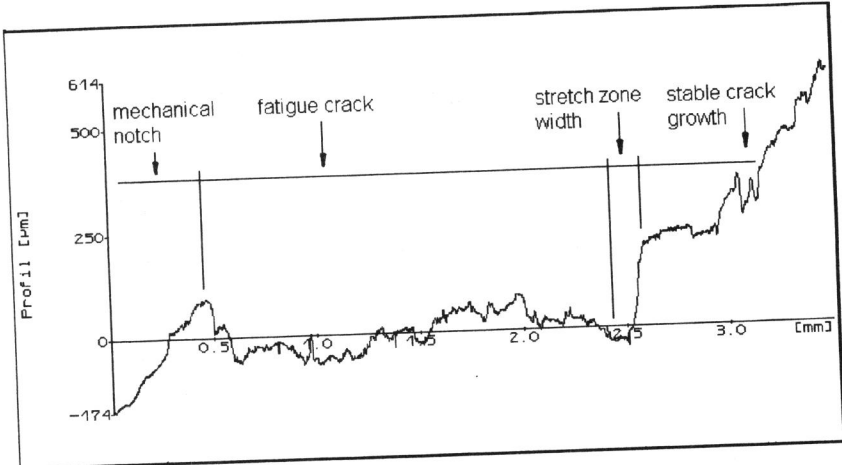


Figure 1 Single profile for analysis of fracture surface topography

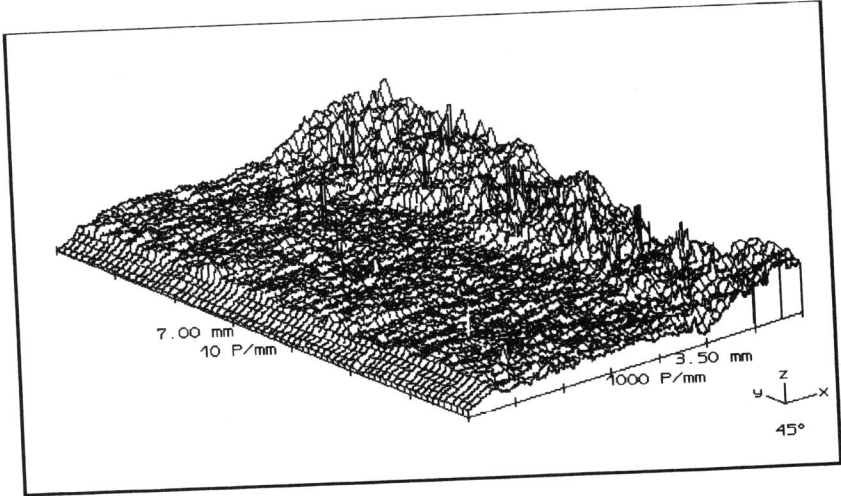


Figure 2 Three dimensional image of a fracture surface

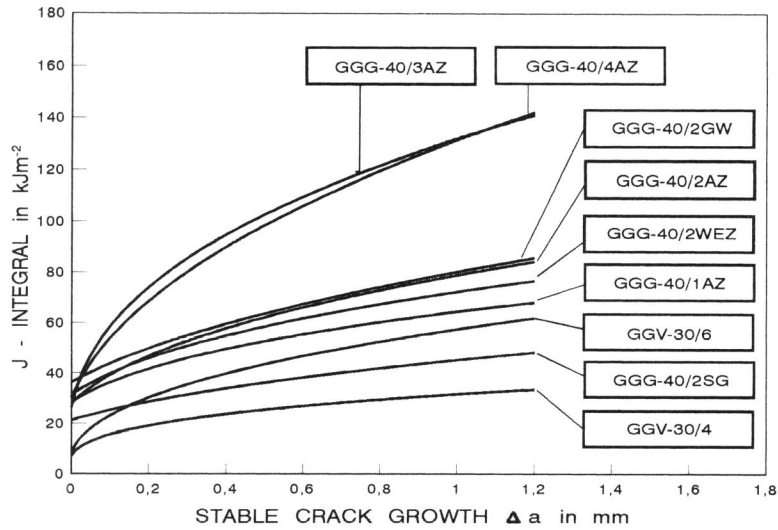


Figure 3 Crack resistance curves of the investigated ferritic cast iron materials

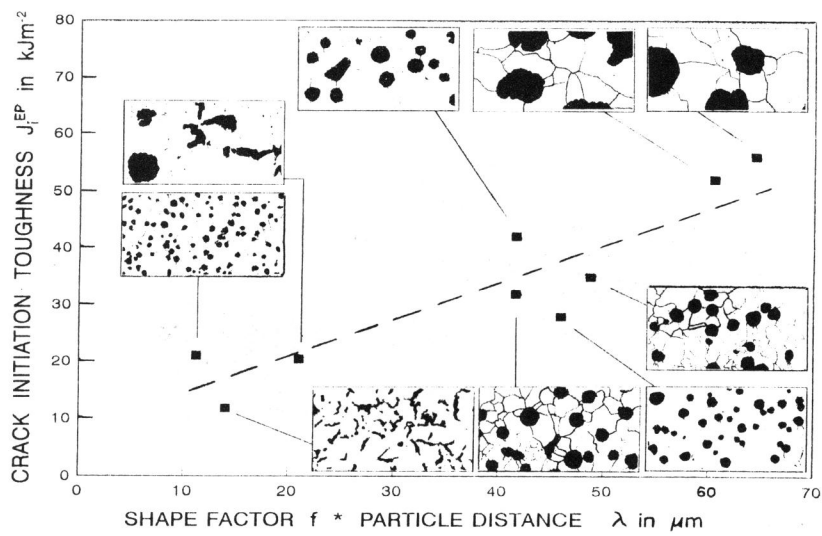


Figure 4 Correlation between crack initiation values of the investigated ferritic cast iron materials and graphite morphology parameters